Breaching or overwash deposition?

Field and model analysis of barrier morphologic response to storms.

Leoni G. H. Heijkers

Master thesis – Earth Surface and Water

Supervisors: 1st dr. ir. Jaap Nienhuis and 2nd prof. dr. Gerben Ruessink

_____

Abstract

Barrier islands are thin and low-lying stretches of land vulnerable to storm impacts. Storms can cause barrier breaching but also washover deposition, these widely different outcomes remain difficult to predict. Here we use the hydrologic and morphologic model, Delft3D, to get an indication of the controlling factors of barrier breaching and washover deposition. We simulate different barrier island morphologies, land cover, and storm characteristics. From the model simulations we found that both an increase in dune height and amount of island development can reduce the breaching potential. The model results are compared against observations from hurricane Sandy. The 24 washovers and 4 breaches that formed during Hurricane Sandy show good agreement with the model results.

_____

Utrecht University

Introduction

Barrier islands are thin stretches of land located parallel to the mainland. They occupy between 6.5 to 12 percent of the world's shorelines (Brenner, Moore, & Murray, 2015; Moore, Patsch, List, & Williams, 2014; Stutz & Pilkey, 2001). Barrier islands are densely populated and provide a number of ecosystem services, including protection of the mainland against storm surges (Grzegorzewski, Cialone, & Wamsley, 2010). Storms have a big impact on barrier islands, as they change sediment volumes. Breaches and washovers are important for longer term change in response to sea-level rise because they generate landward-directed sediment fluxes. On short term however, these are hazards for densely populated places. Both breaches and washovers are very different outcomes and hazards (figure 1). The response to storms is variable alongshore. Sometimes sand deposits in the lagoon, at the back of the island. On other locations island breach and inlets are formed. We still cannot predict when these occur.

Figure 1: Two examples of morphological responses to storms. Left: inlet at Pelican Island (USGS, 2012a)*, right overwash deposition at Pea Island* (USGS, 2012b)*.*

Detailed numerical models exist that can simulate barrier response (e.g. XBeach). But general formative conditions for breaches and overwash deposits are not yet known. For example, the effect

of island width, island height, water level difference between the ocean and the back barrier lagoon, and degree of island development.

The island population on barrier islands is growing (Miselis & Lorenzo-Trueba, 2017), and the frequency of storms increases as well (Landsea, Vecchi, Bengtsson, & Knutson, 2010). It is therefore important to improve the understanding of variability in barrier island response to storms. Here we develop a simplified Delft3D-FLOW model of a barrier island to test different storm conditions and island morphologies and allows for comparison against observed storm impact. Our results will also be valuable as they can be used to parameterize the morphologic impact of storms for long-term models.

Background

2.1 Hydrodynamic impacts on barrier island during storms

Storms initiate changes in hydrodynamics, as the surge level rises. The impacts of storms on barrier islands are categorized by Sallenger (2000). This classification is widely used in research on morphological changes of barrier islands (Plant & Stockdon, 2012; Roelvink, Kessel, Alfageme, & Canizares, 2003). Sallenger (2000) scaled the storm-induced patterns and net erosion/deposition rates into three different regimes. From low to high impact: collision-, overwash-, and inundation-regime (figure 2). This study only looks at the storm impact during the inundation regime. During this regime the low run up elevation (R_{low}) exceeds the dune crest (D_{high}) (figure 2a). The entire
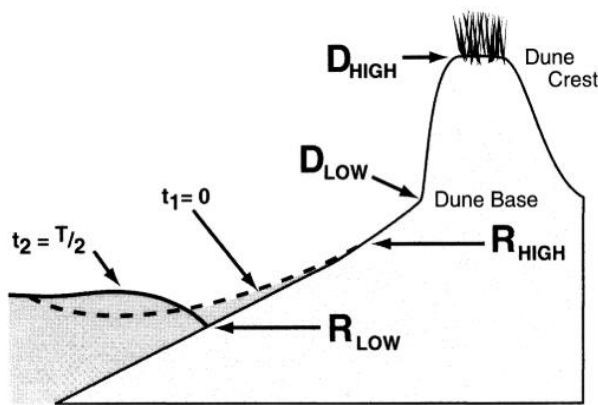

Figure 2a: Definition sketch describing variables used in scaling the impact of storms on barrier islands
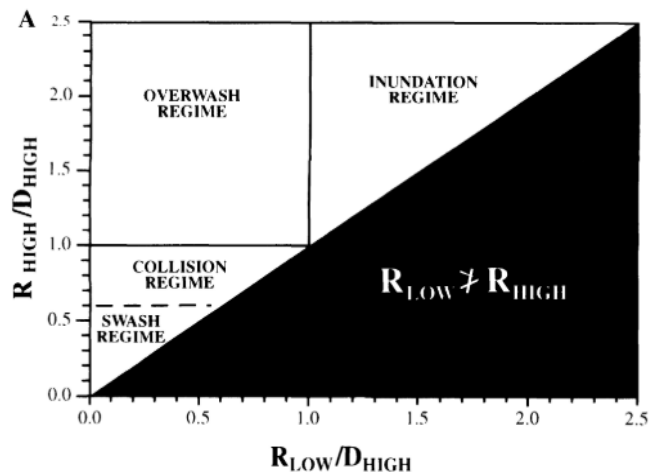
Figure 2b: Delineation of four different regimes categorizing storm impacts (Sallenger, 2000)

island is inundated, including the subaerial part (Sallenger, 2000).

In the inundation regime water flows over the dune crest. This water has a potential energy as there is a difference in hydraulic head between the ocean and the lagoon. This forces the water to flow in the direction of the lagoon. A channel can cut through the island if the flow is channeled and if energy loss due to friction is nihil (Pierce, 1970). A large slope, and therefore a strong flow is created by a large difference in water level and a narrow island width. This water level difference is caused by a time lag between the storm surge at the ocean and the lagoon (McCall et al., 2010; Pirrello, 1992). The duration of the storm determines the period this water level difference will last. The inundation time is also influenced by the barrier island height. High elevated islands experience shorter inundation time than low elevated islands, with the same storm duration (Pilkey Jr., Neal,

Monteiro, & Dias, 1989). McCall et al., (2010) showed that storms with a short duration had less volume change than long lasting storms.

2.2 Morphological impacts on barrier island during the inundation regime

The cross barrier water flow during the inundation regime carries sediment from the island towards the back barrier lagoon. This can result in inlet formation or the deposition of sediment as washover fans (Pierce, 1970). When the flow erodes the dune crest to a height below sea level, the island breaches and an inlet is formed. The ocean and the lagoon are now connected (Oertel, 1985). When the water and sediment flow over the crest of a beach system is more depositional, washover fans are formed (Nienhuis & Lorenzo-Trueba, 2019). When the flow velocity and therefore the carrying capacity is strongly decreased, the sediment deposits. It was seen, by research of Donnelly (2008), that the strongest decrease in overwash flow velocity occurs at the lagoon water level interface. Washovers are therefore often connected to the rear of the island. The thickness of the washover deposit is positively controlled by the accommodation space. This relation causes fan shaped deposits in the back barrier lagoon (Wang & Horwitz, 2006; Matias et al., 2007). When the cross-shore flow is erosional, the breaching potential is increased. If deposition is more dominant the breaching potential is decreased.

Variations in erosion and deposition of barrier island during storms is widely recognized (Elko et al., 2000; Houser, Hapke, & Hamilton, 2008; Stallins, Albert & Parker, 2003). XBEACH is a commonly used model to understand the driving factors causing this variation (Harter & Figlus, 2017; McCall et al., 2010; Van Der Lugt, Quataert, Van Dongeren, Van Ormondt, & Sherwood, 2019; Wesselman et al., 2018). This model is specifically made to simulate dune erosion during extreme wave conditions including wave breaking, surf and swash zone processes. McCall et al. (2010b) found that the water level gradient is one of the most important driving factors for along shore variation in back barrier deposition. Also research by Wesselman et al. (2018) showed that the magnitude of the storm has a high impact on the cross-shore sediment transport.

Barrier island characteristics can also force along shore variation in storm response. If an island is high and wide the chance of inlet formation is minimized (Claudino-Sales, Wang, & Horwitz, 2008; Clinch, Russ, Oliver, Mitasova, & Overton, 2012; Kraus, Militello, & Todoroff, 2002; Stone, Liu, Pepper, & Wang, 2004). The influence of island cover differences on barrier island response was investigated by Rogers et al. (2015). A comparison of prestorm and poststorm Lidar images showed

that areas with a high building density experienced limited erosion and deposition compared to natural areas. McCall et al. (2010) found that resistance to erosion of the island cover had larger impacts on the sediment transport during storms, than hydraulic forces as water level difference and wave height.

Table 1: Hypothesized effect of variables on inlet and washover formation (negative (-), positive (+)).

	Breaching potential	Overwash potential
Island height	-	+
Island width	-	+
Water level difference	+	-
Storm duration	+	-
Island cover	-	+

2.3 Hurricane Sandy impact

Hurricane Sandy was one of the most devastating hurricanes of the last decade. It was a post-tropical cyclone when it made landfall on October 29th 2012 at 23:30 UTC, near Brigantine, New Jersey (N.J.). With an estimated damage of $50 billion, it was the costliest hurricane since 1900 (Blake, Kimberlain, Berg, Cangialosi, & Beven, 2013). At Sandy Hook, N. J. a water level of 2.71m was measured on normally dry land. During the storm large scale erosion of beaches and dunes took place, along the east coast of the United States. Dune crest at Fire Island experienced extreme erosion and lost 54.4% of their original volume. The island breached at three locations (Hapke et al., 2013).

Method

3.1 Model setup

The model used in this research is DELFT3D-FLOW. This model combines hydrodynamic and morphodynamic equations to simulate shallow water flow and sediment transport in three dimensions. The set of equations that is being used contains: horizontal momentum equations, the continuity equation, the Van Rijn formulations for sediment transport (1993), and a turbulence closure model. The bathymetry updates every time step (Deltares, 2014; Lesser, Roelvink, van Kester, & Stelling, 2004). The DELFT3D module is a commonly used tool to simulate flow in shallow waters. Examples of research areas are: water levels in coastal areas (Stockdon, Sallenger, Holman, & Howd, 2007), barrier islands (Roelvink et al., 2003), rivers (Nienhuis, Törnqvist, & Esposito, 2018), and shallow seas (Luijendijk, 2001).

The input grid for the model has a size of 1x1 km, with two water bodies (ocean and lagoon) and one barrier island. The bottom profile is highest on top of the barrier (5m), and lowers linearly from the back shore to the end of the lagoon (-3m) (figure 3). In the middle of the barrier island the maximum height is reduced to initiate a breach. The cell size varies from 50x50 m in the breach, 50X100 m directly behind the breach and on the island, and 100X100 m in the rest of the lagoon (figure 3). Over the entire grid a randomness 5% in surface height is added, to get more asymmetrical washover geometries. The grid boundaries are closed in the x-direction and open in the y-direction. Water comes in at x = 0 and leaves the model at x = 140. Water and sediment can
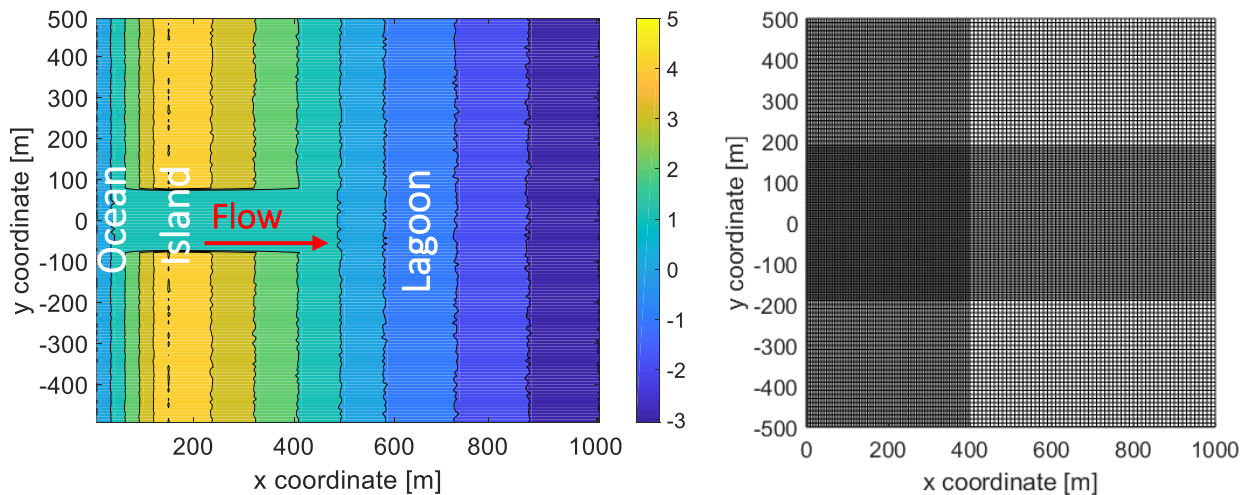

Figure 3: left: Bottom depth [m], right: morphological grid.

flow out of the model. For the bottom roughness we use a uniform Chezy roughness value of 65 in the U- and V- direction [$m^{1/2}$/s].

3.2 Tested variables

Island height

To simulate the effect of island height on barrier island response to storms, the breach height is varied. This area of 100m in the middle of the barrier represents a local lowering in the dune crest. The elevation of this part of the island is varied between 1 and 2 meter.

Water level slope and storm duration

Every model run started with an equal water level in both water bodies. The flow is initiated by an elevation of the water level on the ocean side of the barrier. Figure 4 shows an example water level series at the ocean side of the barrier with a maximum height of 2.5m. The water level in the lagoon remained constant over time. This created a water level difference during the storm. The maximum water level difference varied from 2.1 to 4.9 m. Because of this water level difference, water starts to flow with a certain speed through a breach, and created deposition and erosion. The duration of the high water peak is varied between runs. The shortest storm simulation had a period of 3 hours and the maximal storm duration was 24 hours. High water peaks of 6, 9, 12 and 18 hours have been watched. All simulations developed with time steps of 20 minutes.
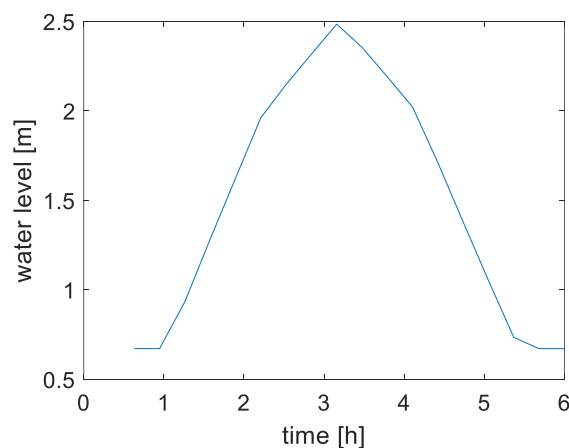

Figure 4: Water level at the ocean side of the barrier over time.

The island width also has influence on the water level slope. The domain length is kept constant, so an increase in width decreases the slope. Two islands with a different width are used in the simulations. The narrow island has a width of 200m and the wide island has a width of 400m.

Island cover

In this study two types of island cover are differentiated: sand and asphalt. For the category 'sand' we use non-cohesive sediment with a median sediment diameter of $200\,\mu m$. To simulate the asphalt cover, a layer of 0.1 m cohesive sediment is added to the initial grid (figure 4). For this layer the critical bed shear stress for erosion is set to 1.0e+1 [N m^{-2}]. The cohesive sediment is only placed on the back side of the dune crest to make it possible for the beach to erode. Figure 5 shows the location of the asphalt layer for both island widths.
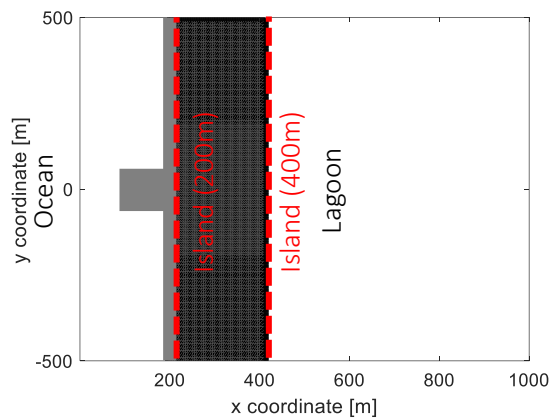
Figure 5: Island back shore in red. Asphalt layer for 200m island width (grey) and 400m island width (grey

3.3 Model output

We have analyzed the morphological change by looking at the difference in bottom depth over time. The volumetric difference results in deposition and erosion cells. The Delft3D output is classified as inlet when the summed erosion exceeds the summed deposition. We have classified a model result as overwash when the total deposition is larger than the erosion. The erosion and deposition volumes are obtained from the lagoon area directly connected to the backbarrier. When an inlet is formed still a lot of sediments can be deposited in the back of the lagoon, without connection to the island. This can disrupt the storm output classification. Therefore, the sediment volumes are measured from a lagoon area directly connected to the island and with a limited extend into the lagoon (appendix 1.1).

3.4 Statistical analysis

The four variables: breach height; water level slope; storm duration; and island cover are varied with the values in table 2. The influence of the variables on (E) and (D) is statistically tested with the student t-test. The p-values are assessed at a 0.05 significance level.

Table 2: Variable values

Variable	value				
Island height [m]	1	2			
Storm duration [m]	6	9	12	18	24
Water level difference [m]	2.5	3	3.5	4.5	
Island width [m]	200	400			
Island cover	sand	asphalt			

3.5 Comparison to Sandy observations

We have compared the Delft3D-model results to observed breaches and overwash deposits from hurricane Sandy data. With this comparison the model performance could be estimated. From NOAA Rapid Response Imagery (NOAA, 2012) we have found 6 breaches and 24 overwash fans along the New Jersey coast and Fire Island, New York (appendix 3).

We have used pre-storm Google Earth images and topography to extract island width for these locations. The pre-storm island height has been extracted from the Scenario-based coastal change forecasts: Elevation of the dune crest dataset. This dataset provides the height of the dune crest (DHIGH in m, NAVD88) for the East coast of the United States. The elevation has been extracted from LIDAR (Light Detection and Ranging) topography with a resolution of 10 m along shore and 2.5 m cross-shore, and averaged into 1 km bins. The data was collected between May and June 2010, by the US Army Corps of Engineers (USACE, 2010). The prestorm island height of the analyzed locations is 5m on average.

We have retrieved hurricane Sandy ocean and lagoon water levels from an ADCIRC hindcast model simulation via the Coastal Emergency Risk Assessment (Coastal Emergency Risks Assessment, n.d.). This simulation show that the water level differences between the ocean and lagoon ranged from 0 to 3.7m for the different locations. Because ADCIRC model results exist up

to the peak of the storm, we extract storm duration from measurements of the nearest NOAA tide gauge stations (Forbes, Rhome, Mattocks, & Taylor, 2014). The length of the peak storm surge is taken as the storm duration. The dominant prestorm island cover was optained from the Google Earth Engine Timelapse, which contains Landsat images from 2011 (Google Earth Engine, n.d.).

Results

4.1 Model output

We ran 144 simulations for different island geometries and storm characteristics (table 2). The simulations in which the model became unstable are not included in the analysis. The unstable runs contain simulations which ended with unrealistic bottom depths and heights, below 10m (Dias, Ferreira, Matias, Vila-Concejo, & Sá-Pires, 2003) and above 5m (appendix 2.2). The 95 stable runs resulted in 23 inlets, 41 washovers, and 32 situations with no change or a little back shore
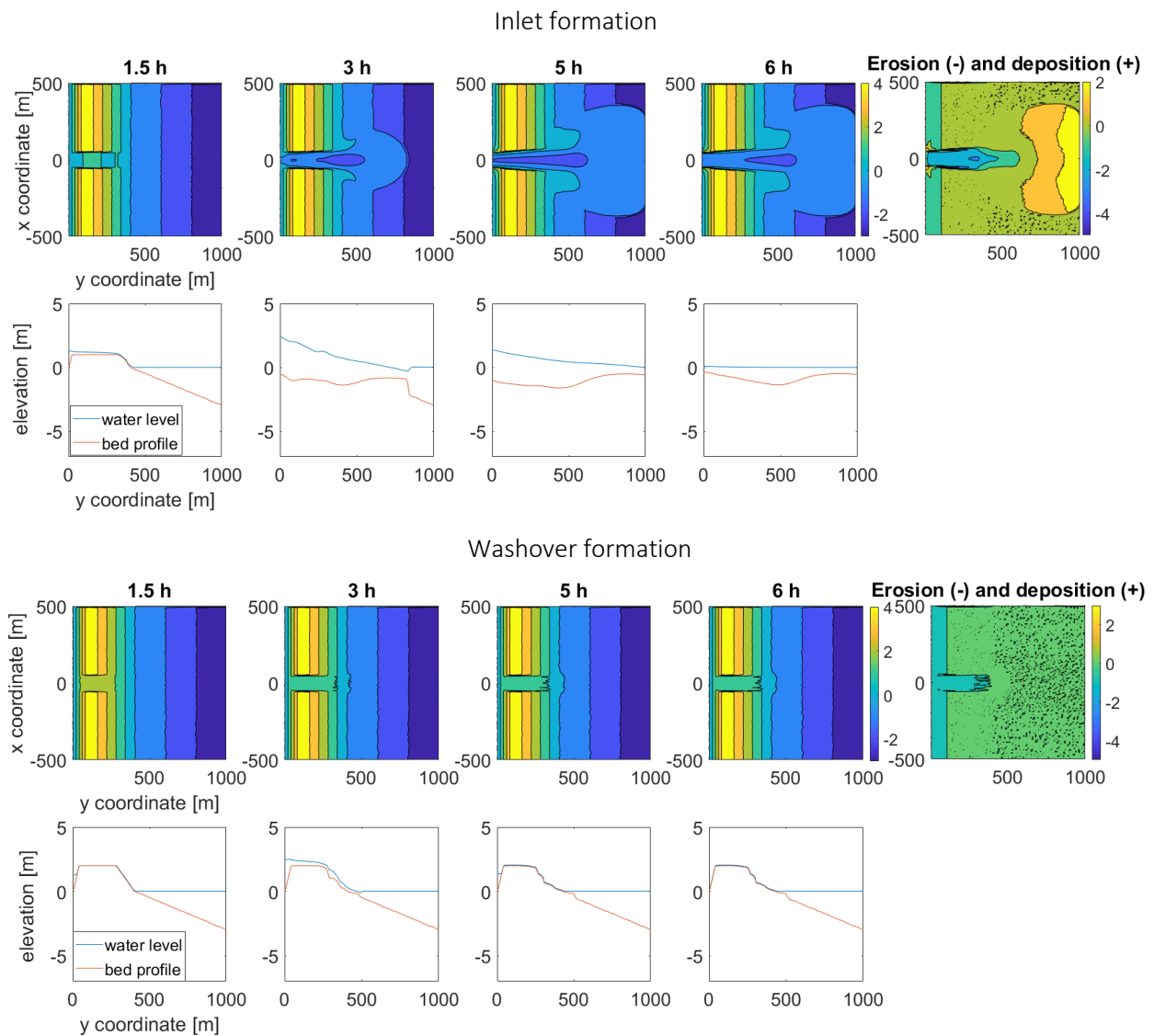
Figure 2: Evolution of bed level in two runs with same boundary conditions, only different island heights. Top: 1m island height, Bottom: 2m island height

erosion, based on the area above sea level. When we classify the model output on deposition minus erosion the simulations result in 22 inlets and 73 washovers. Figure 5 shows the bottom depth evolution of two different runs resulting in an inlet and washover.

4.2 Influence of tested variables on barrier island response to storms

Impact of the barrier island height

In figure 6 we compare 42 simulations with a 1m island height to 53 simulations with an elevation of 2m. We find that increasing the island height from one to two meter results in more deposition than erosion. 40% of the 1m simulations showed more erosion than deposition. The simulations with a 2m elevation ended in for 7.5% in net erosion. We also see that the summed displaced sediment volume (D-E) with an island elevation of 2m, is less extreme than in the lower situation. The standard deviation of the 1m simulations (3.7e+04) is much higher than the standard deviation

Figure 6: Deposition - erosion categorized on island height

Figure 7: Water slope for inlets and washovers

Figure 8: Deposition - erosion with varying storm duration

Figure 9: Deposition - erosion categorized on island cover

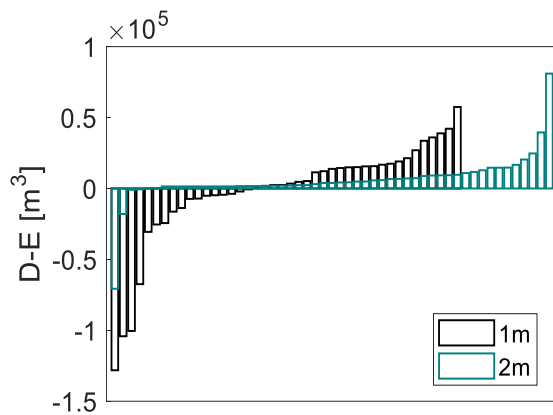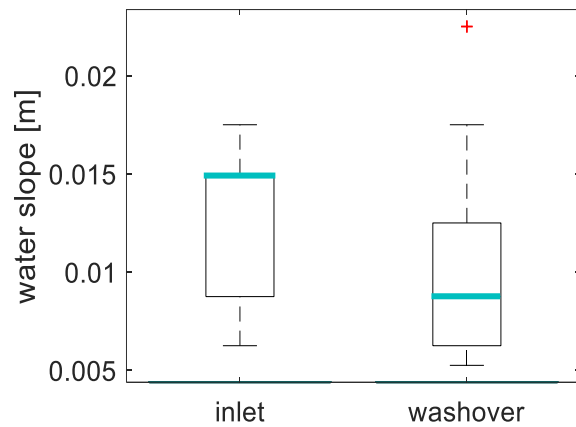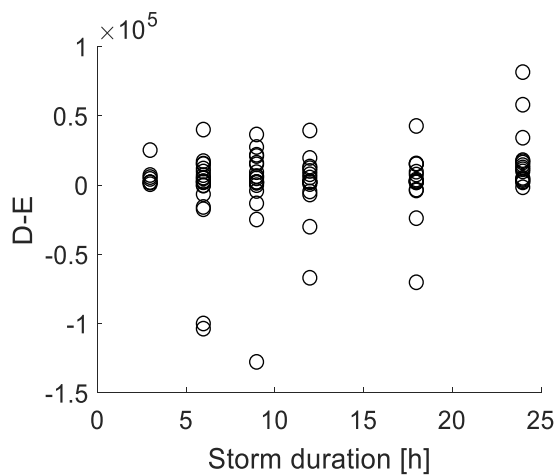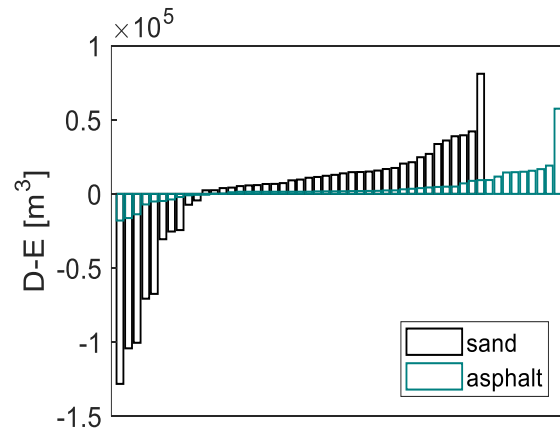of the 2m simulations (1.7e+04). This tells us that a higher elevation results in a lower variability in net sediment change. The total amount of runs, stable and unstable, has 72 simulations with 1m and 72 simulations with 2m island heights. When we look at only the stable runs, we see that the simulations with a height of 2m ended more often stable than the simulations with 1m elevation. Figure 6 shows more simulations for the 2m island height.

Impact of the water level slope

The influence of the water slope is visualized in figure 7. The inlet box is positioned higher than the washover box. Therefore, it is more likely that an inlet will form with higher water slopes. The median of the inlet box exceeds the washover box, which tells us that a higher slope is more often related to inlet than washover formation. It can be seen from figure 7, that the boxplot for inlet is positive skewed and for washover almost normal distributed. The boxes have an overlap, which means that between slopes of 0.008-0.0125m both inlets and washovers form.

Impact of the storm duration

The relation between the summed displaced sediment volume and the storm duration can be seen in figure 8. We don't find a relation between the storm duration and the net sediment change.

Impact of the island cover

In figure 9 we compare 43 runs with a sand cover to 52 runs with an asphalt cover. It can be seen that increasing the critical shear stress results less extreme D-E values, both negative and positive. The standard deviation of the sand cover simulations (4e+04) is much higher than the standard deviation of the asphalt cover simulations (1e+04). 23% of the sand cover simulations resulted in a negative net sediment change. For the asphalt cover simulations this is 21%, but the net erosion is much smaller than for the sand cover simulations. We also see that runs including an asphalt layer ended more stable than without this layer, as the number of asphalt runs in figure 9 is more than the number of sand covered runs.

Influence of island morphology and storm characteristics on breach probability

The relation between the different variables and the storm output (inlet or washover formation) has been analyzed with a t-test. Table 3 shows the output of the t-test. We see that at only the island height is significant at a 0.05 and even 0.01 level. Storm duration, water level slope, and island

cover do not have a statistical significant relation with the storm output. The water level slope has no significant relation due to the large overlap of the output boxes in figure 7. For the storm duration, there is no significant relation, because there is no relation found in figure 8. The island cover does have a large influence on the sediment changes during the storm, as the amount of net displaces is dramatically reduced (figure 9). However, the chance of inlet formation does not change with a different cover.

Table 3: t-test p-values for tested variables and model output

Variable	p-value
height	7.7622e-05
slope	0.264
duration	0.238
cover	0.808

4.3 Model comparison against hurricane Sandy

Comparison of the modeled and observed washover fan size

The 24 Sandy overwash fan sizes are defined as the new deposited sand area above sea level. The observations show a negative relation between the fan size of the overwash fan and island height (figure 10). The formation of large overwash fans is more often found at low elevated island, than with high elevated islands. No relation can be found between water slope and fan size. Also the storm duration shows no clear relation with fan size. However, the island cover does show a negative relation. The fan size from Sandy observations with an asphalt island cover are smaller than the fans with a sand cover, except for one asphalt observation.

When we look at the modeled fan sizes in figure 10, the deposited area is 100 times as large as the observed ones. The relation between the island height and the fan size of the model shows the same pattern as the Sandy observations. Low elevated islands more often result in large overwash fans, than high elevated islands. Also the water slope has no clear relation with the fan size, as the observations show. This lack of relation also applies for the storm duration and fan size. Even as the observations, the modeled fan sizes with a sand cover are much larger than the with an asphalt cover.
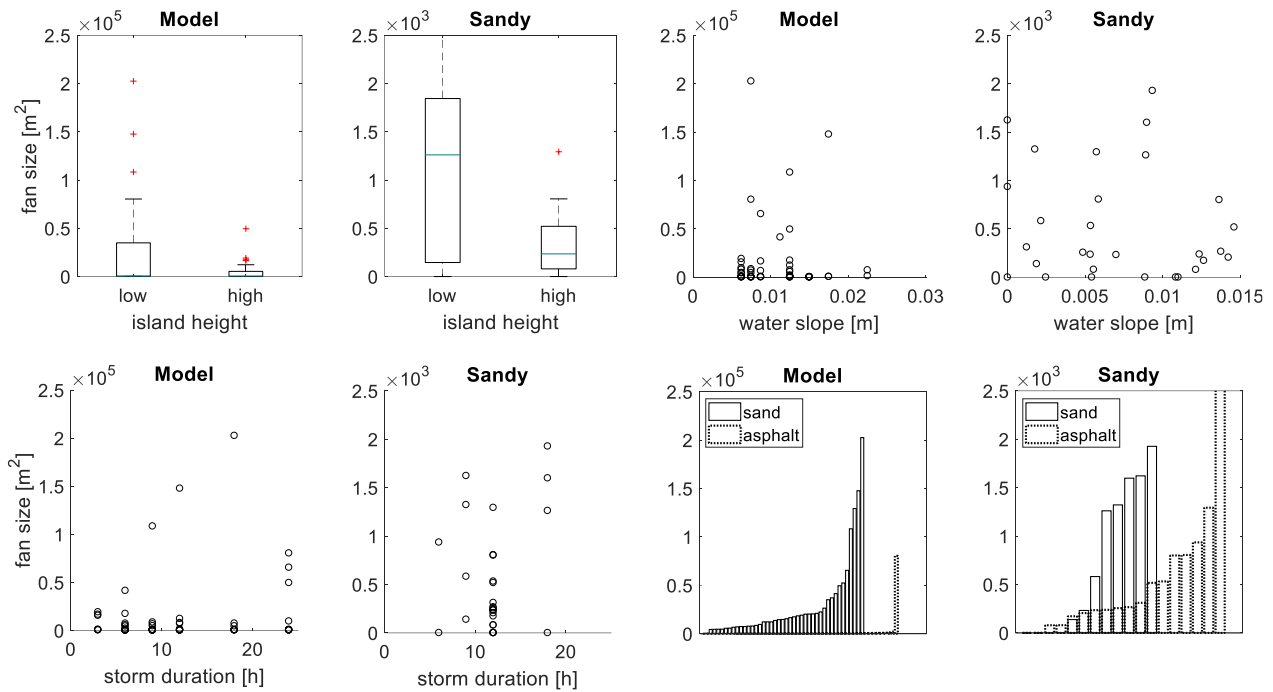
Figure 10: Relation between tested variables and fan size [m2] for the model and Sandy observations

Comparison of the modeled and observed storm output

The 30 Sandy observations contain 24 washovers and 6 inlets. The influence of the island and storm characteristics and their relation with storm output are shown in table 4. The differentiation between high and low elevation and slope, and long and short duration is made at the average value. For example, the average island height was 5m, so below 5m was classified as low elevated and above 5m as high. It can be seen that high islands more often resulted in a washover than an inlet, than low elevated island. The influence of high water level slope on storm output is less visible, as these percentages do not differ much. Also, no relation be found between the storm duration and storm output. The island cover, on the other hand shows a strong influence. The asphalt covered islands show less inlets than island with a sand cover.

When we compare these observed outcomes to the modeled storm outputs, we see similar relations. The simulations with a low island height resulted more often in inlets, compared to the low island high islands. The difference in storm output between low and high water slopes is larger in the model than from the observations, but both have a positive relation with breaching potential. For the storm duration there is a difference in storm output visible, in contrast to the Sandy

16

observations. Storms with a long durations resulted more often in washovers than storms with a short duration. The island cover showed almost no difference in storm output in the model, which is not similar compared to the observations.

Table 4: Storm output in % from the model and Sandy observations per variable

Island height				
	Model		Sandy	
inlet	19%	7.5%	23%	18%
washover	81%	93.5%	77%	82%
	low	high	low	high

Water slope				
	Model		Sandy	
inlet	18%	27%	19%	21%
washover	82%	73%	81%	79%
	low	high	low	high

Storm duration				
	Model		Sandy	
inlet	23%	15%	17%	17%
washover	77%	85%	83%	83%
	short	long	short	long

Island cover				
	Model		Sandy	
inlet	23%	21%	33%	11%
washover	77%	79%	67%	89%
	sand	asphalt	sand	asphalt

Discussion

Although the model is a highly simplified version of reality, it gives an indication of the importance of certain variables in barrier island response to storms. The results show that with an increase in island elevation barrier island breaching is less likely than washover formation. This is in line with the outcomes of prior research (Claudino-Sales et al., 2008; Clinch, Russ, Oliver, Mitasova, & Overton, 2012; Kraus et al., 2002; Stone et al., 2004). The decrease of breaching potential can be explained by the larger volume of sediment that has to be eroded. Higher islands contain a larger sediment volume than low elevated islands. The expected positive influence of island height on washover potential can also be seen from the results. The modeled net D-E volumes are smaller both in the negative and positive side. This can be declared by the fact that high elevated islands experience shorter inundation times than low elevated islands, when the storm duration is the same.

The influence of the water slope is less clear from the results than was hypothesized. This can be caused by the fact that only a small amount of runs with a large water level difference ended up being stable. The unstable runs mainly contain 3.5m water level difference and higher (appendix 2.2). Therefore, this group is not well represented in the analysis which creates a negative bias on the breach potential from the model. The model output is in line with the Sandy observations.

From the storm duration model output no clear relation can be seen. This doesn't fit the hypnotized positive effect. This may be caused by time scale on which morphological responses to storms take place. When they inlets and washovers form in the first few hours of the storm, increasing the duration of the storm doesn't have an influence anymore. Changing the island cover doesn't show differences on both the breaching and washover potential. This is against expectations and not in line with the observations from Sandy, as these indicated that the amount of inlets would reduce with an asphalt cover. This can be caused by the absence of many sand cover simulations, as they are dominant in the unstable runs. Both the negative and positive D-E values were strongly reduced. This can be declared by the increase in resistance to erosion when an asphalt layer is added.

The modeled fan sizes and sediment volumes cannot be used for predictions, as these seem unrealistically large, when comparing it to the Sandy data. On the other hand, the influence of the different variables on the fan size does show same patterns between the model and Sandy observations. Which indicates that the model can be used to get a better understanding of the controlling factors of barrier island response to storms.

The difference in fan size could be reduced by changing the island cover in the model, as this has a large effect on the net changes in sediment volumes. From the Landsat images (Google Earth Engine, n.d.) it can be seen that these covers are much more complex and variable than was assumed in this research.

For the comparison with hurricane Sandy the storm duration was obtained from NOAA tide gauges. As the distance between these stations is quite large in the study area, the storm duration could differ from reality at some transects. The validation with the Sandy data can also be influenced by the determination of the island cover. The island cover at the transact location is visually categorized from satellite images. In this classification only two categories were used, but at many locations it wasn't just one category. The most dominant cover type was chosen. In future research more types could be added, to be able to also include the influence of vegetation and mixed island covers. In addition, other, more storm specific variables could be added, such as distance to landfall, wave and wind characteristics. According to Billson, Russell, & Davidson (2019), infragravity waves are the main cause of beach and dune erosion. Therefore, it would be good to include these in further research. To include these variables another model should be used.

Conclusion

In this study we looked at the controlling factors behind difference in barrier island response to storms. We used an Delft3D-FLOW model to simulate inlet and washover formations and compared these to Hurricane Sandy observations. We simulated different storms and pre-storm barrier island conditions, the island height, width and cover, even as the water level difference and storm duration. The model and Sandy results show resemblance. From both the model simulations and the Sandy observations we found that an increase in island height reduces the breaching potential. Also the island cover has influence on the breaching potential. When asphalt is added to the island surface we see reduction of inlets formation from the Sandy observations and a decrease in the amount of eroded and deposited sediment in the model. Both the island height and island cover increase the chance of washover formation during inundation. The water slope and the storm duration don't show a clear influence on storm output.

References

Billson, O., Russell, P., & Davidson, M. (2019). Storm waves at the shoreline: When and where are infragravity waves important? *Journal of Marine Science and Engineering*, *7*(5). https://doi.org/10.3390/jmse7050139

Blake, E. S., Kimberlain, T. B., Berg, R. J., Cangialosi, J. P., & Beven, J. L. (2013). *Tropical Cyclone Report - Hurricane Sandy*.

Brenner, O. T., Moore, L. J., & Murray, A. B. (2015). The complex influences of back-barrier deposition, substrate slope and underlying stratigraphy in barrier island response to sea-level rise: Insights from the Virginia Barrier Islands, Mid-Atlantic Bight, U.S.A. *Geomorphology*, *246*, 334–350. https://doi.org/10.1016/j.geomorph.2015.06.014

Claudino-Sales, V., Wang, P., & Horwitz, M. H. (2008). Factors controlling the survival of coastal dunes during multiple hurricane impacts in 2004 and 2005: Santa Rosa barrier island, Florida. *Geomorphology*, *95*(3–4), 295–315. https://doi.org/10.1016/j.geomorph.2007.06.004

Clinch, A. S., Russ, E. R., Oliver, R. C., Mitasova, H., & Overton, M. F. (2012). Hurricane Irene and the Pea Island Breach: Pre-storm site characterization and storm surge estimation using geospatial technologies. *Shore & Beach*, *80*(2), 38–46.

Coastal Emergency Risks Assessment. (n.d.). ADCIRC storm sturge and wave guidance - SANDY. Retrieved October 6, 2019, from http://cera.coastalrisk.live/

Deltares. (2014). Delft3D 3D-FLOW user manual version 3.15.34158. Delft, Netherlands. Retrieved from www.delftsoftware.com

Dias, J., Ferreira, Ó, Matias, A., Vila-Concejo, A., & Sá-Pires, C. (2003). Evaluation of Soft Protection Techniques in Barrier Islands by Monitoring Programs: Case Studies from Ria Formosa (Algarve-Portugal). Journal of Coastal Research, 117-131.

Donnelly, C. (2008). *Coastal overwash : processes and modelling*. Water Resources Engineering, Lund University.

Elko, N. A., Sallsngsr, A. H., Elko, N. A., Sallenger, A. H., Guy, K., & M Morgan, K. L. (2000).

Barrier island elevations relevant to potential storm impacts: 1. Techniques, USGS Open File Report 02-287. Journal of Coastal Research (Vol. 33701). Retrieved from http://coastal.er.usgs.gov/hurricanes

Forbes, C., Rhome, J., Mattocks, C., & Taylor, A. (2014). *Predicting the storm surge threat of hurricane sandy with the national weather service SLOSH model*. *Journal of Marine Science and Engineering* (Vol. 2). https://doi.org/10.3390/jmse2020437

Google Earth Engine. (n.d.). Google Earth Timelapse. Retrieved October 14, 2019, from http://earthengine.google.com/timelapse/#v=40.72855,-72.8712,11.973,latLng&t=2.06

Grzegorzewski, A. S., Cialone, M. A., & Wamsley, T. V. (2010). Interaction of Barrier Island and Storms: Implications for Flood Risk Reduction in Louisiana and Mississippi. *Journal of Coastal Research*, (59), 156–164.

Hapke, C. J., Brenner, O., Hehre, R., Reynolds, B., Jewell, S., Kimball, S. M., & Director, A. (2013). *Coastal Change from Hurricane Sandy and the 2012-13 Winter Storm Season: Fire Island, New York Open-File Report 2013-1231*. Retrieved from http://store.usgs.gov

Harter, C., & Figlus, J. (2017). Numerical modeling of the morphodynamic response of a low-lying barrier island beach and foredune system inundated during Hurricane Ike using XBeach and CSHORE. *Coastal Engineering*, *120*, 64–74. https://doi.org/10.1016/j.coastaleng.2016.11.005

Houser, C., Hapke, C., & Hamilton, S. (2008). Controls on coastal dune morphology, shoreline erosion and barrier island response to extreme storms. *Geomorphology*. https://doi.org/10.1016/j.geomorph.2007.12.007

Kraus, N., Militello, A., & Todoroff, G. (2002). Barrier Breaching Processes and Barrier Spit Breach, Stone Lagoon, California. *Shore and Beach*, *70*.

Landsea, C. W., Vecchi, G. A., Bengtsson, L., & Knutson, T. R. (2010). Impact of Duration Thresholds on Atlantic Tropical Cyclone Counts. *Journal of Climate*, *23*(10), 2508–2519. https://doi.org/10.1175/2009JCLI3034.s1

Lesser, G. R., Roelvink, J. A., van Kester, J. A. T. M., & Stelling, G. S. (2004). Development and validation of a three-dimensional morphological model. *Coastal Engineering*, *51*(8–9), 883–

915. https://doi.org/10.1016/j.coastaleng.2004.07.014

Luijendijk, A. (2001). *Validation, calibration and evaluation of Delft3D-FLOW model with ferry measurements*. Retrieved from https://www.researchgate.net/publication/27352164

McCall, R. T., Van Thiel de Vries, J. S. M., Plant, N. G., Van Dongeren, A. R., Roelvink, J. A., Thompson, D. M., & Reniers, A. J. H. M. (2010). Two-dimensional time dependent hurricane overwash and erosion modeling at Santa Rosa Island. *Coastal Engineering*, *57*(7), 668–683. https://doi.org/10.1016/j.coastaleng.2010.02.006

Miselis, J. L., & Lorenzo-Trueba, J. (2017). Natural and Human-Induced Variability in Barrier-Island Response to Sea Level Rise. *Geophysical Research Letters*, *44*(23), 11,922-11,931. https://doi.org/10.1002/2017GL074811

Moore, L. J., Patsch, K., List, J. H., & Williams, S. J. (2014). The potential for sea-level-rise-induced barrier island loss: Insights from the Chandeleur Islands, Louisiana, USA. *Marine Geology*, *355*, 244–259. https://doi.org/10.1016/j.margeo.2014.05.022

Nienhuis, J. H., & Lorenzo-Trueba, J. (2019). Simulating barrier island response to sea-level rise with the barrier island and inlet environment (BRIE) model v1.0. *Geoscientific Model Development Discussions*, (March), 1–33. https://doi.org/10.5194/gmd-2019-10

Nienhuis, J. H., Törnqvist, T. E., & Esposito, C. R. (2018). Crevasse Splays Versus Avulsions: A Recipe for Land Building With Levee Breaches. *Geophysical Research Letters*, *45*(9), 4058–4067. https://doi.org/10.1029/2018GL077933

NOAA, N. O. and A. A. (2012). Hurricane Sandy: Rapid Response Imagery of the Surrounding Regions. Retrieved September 22, 2019, from http://geodesy.noaa.gov/storm_archive/storms/sandy/index.html#

Oertel, G. F. (1985). THE BARRIER ISLAND SYSTEM. *Marine Geology*, *63*, 1–18.

Pierce, J. W. (1970). TIDAL INLETS AND WASHOVER FANS. *Journal of Geology*, *78*, 230–234. Retrieved from http://www.journals.uchicago.edu/t-and-c

Pilkey Jr., O. H., Neal, W. J., Monteiro, J. H., & Dias, J. M. A. (1989). Algarve Barrier Islands: A Noncoastal-Plain System in Portugal. *Journal of Coastal Research*, *5*(2), 239–261.

Pirrello, M. A. (1992). *THE ROLE OF WAVE AND CURRENT FORCING IN THE PROCESS OF BARRIER ISLAND OVERWASH*.

Plant, N. G., & Stockdon, H. F. (2012). Probabilistic prediction of barrier-island response to hurricanes. *Journal of Geophysical Research: Earth Surface*, *117*(3). https://doi.org/10.1029/2011JF002326

Roelvink, J. A., Kessel, T. Van, Alfageme, S., & Canizares, R. (2003). Modelling of Barrier Island Response To Storms. *The Fifth International Symposium on Coastal Engineering and Science of Coastal Sediment Processes, Coastal Sediments '03*, (January). Retrieved from http://eprints.utas.edu.au/4774/

Rogers, L. J., Moore, L. J., Goldstein, E. B., Hein, C. J., Lorenzo-Trueba, J., & Ashton, A. D. (2015). Anthropogenic controls on overwash deposition: Evidence and consequences. *Journal of Geophysical Research F: Earth Surface*, *120*(12), 2609–2624. https://doi.org/10.1002/2015JF003634

Sallenger, A. H. J. (2000). Storm impact scale for barrier islands. *Journal of Coastal Research*, *16*(3), 890–895.

Stallins & Albert, A., & Parker, J. J. (2003). The Influence of Complex Systems Interactions on Barrier Island Dune Vegetation Pattern and Process. *Annals of the Association of American Geographers*, *93*(1), 13–29. https://doi.org/10.1111/1467-8306.93102

Stockdon, H. F., Sallenger, A. H., Holman, R. A., & Howd, P. A. (2007). A simple model for the spatially-variable coastal response to hurricanes. *Marine Geology*, *238*(1–4), 1–20. https://doi.org/10.1016/j.margeo.2006.11.004

Stone, G. W., Liu, B., Pepper, D. A., & Wang, P. (2004). The importance of extratropical and tropical cyclones on the short-term evolution of barrier islands along the northern Gulf of Mexico, USA. *Marine Geology*, *210*(1–4), 63–78. https://doi.org/10.1016/j.margeo.2004.05.021

Stutz, M. L., & Pilkey, O. H. (2001). A Review of Global Barrier Island Distribution. *Journal of Coastal Research*, (34).

USACE, U. A. C. of E. (2010). Joint Airborne Lidar Bathymetry Technical Center of Expertise

Southeast Lidar: Florida, Georgia, South Carolina, North Carolina form 2010-06-15 to 2010-08-15. NOAA National Centers for Environmental Information. Retrieved from https://inport.nmfs.noaa.gov/inport/item/50093

USGS. (2012a). Oblique aerial photographs of Pelican Island and Fire Island, New York. Retrieved January 3, 2020, from https://www.usgs.gov/media/images/oblique-aerial-photographs-pelican-island-and-fire-island-new-york

USGS. (2012b). Oblique aerial photographs of Pea Island National Wildlife Refuge. Retrieved January 10, 2020, from https://www.usgs.gov/media/images/oblique-aerial-photographs-pea-island-national-wildlife-refuge

Van Der Lugt, M. A., Quataert, E., Van Dongeren, A., Van Ormondt, M., & Sherwood, C. R. (2019). Morphodynamic modeling of the response of two barrier islands to Atlantic hurricane forcing. https://doi.org/10.1016/j.ecss.2019.106404

Wang, P., & Horwitz, M. H. (2006). Erosional and depositional characteristics of regional overwash deposits caused by multiple hurricanes. *Sedimentology*, *54*(3), 545–546. https://doi.org/10.1111/j.1365-3091.2006.00848.x

Wesselman, D., de Winter, R., Engelstad, A., McCall, R., van Dongeren, A., Hoekstra, P., … van der Vegt, M. (2018). The effect of tides and storms on the sediment transport across a Dutch barrier island. *Earth Surface Processes and Landforms*, *43*(3), 579–592. https://doi.org/10.1002/esp.4235

Appendix 1

Figure 1.   Lagoon area with most representative D-E output, compared to the storm output based on the area above water.
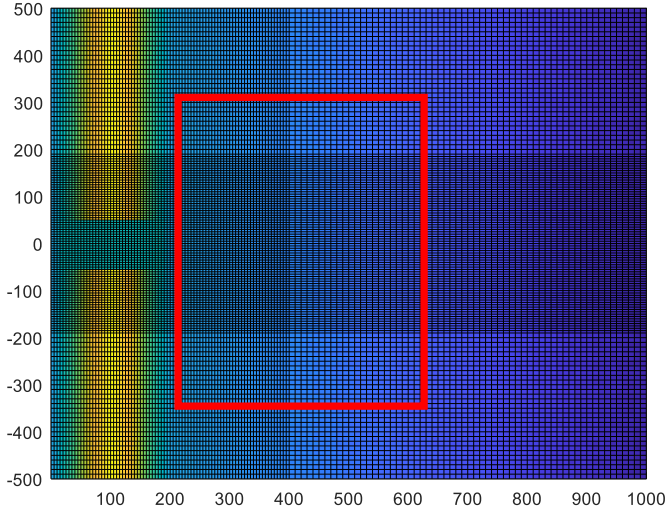
Figure 2.   Model output with D-E based on the red box, and colored with the visualization output.
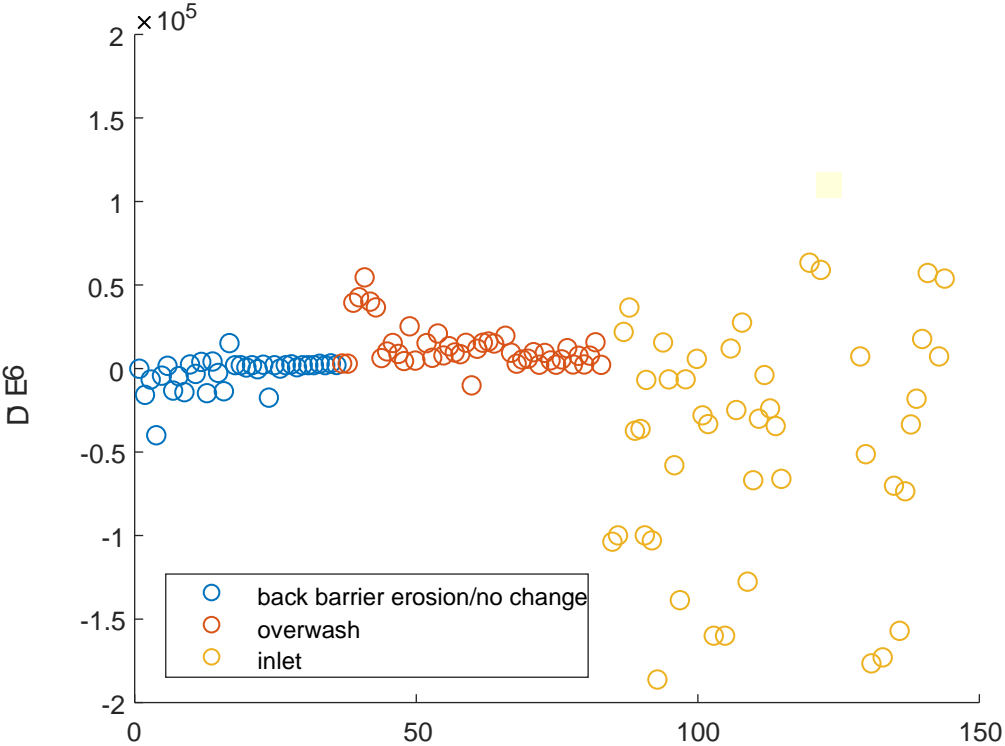
Figure 3.   Model output form figure 3 with excluded runs (errors)
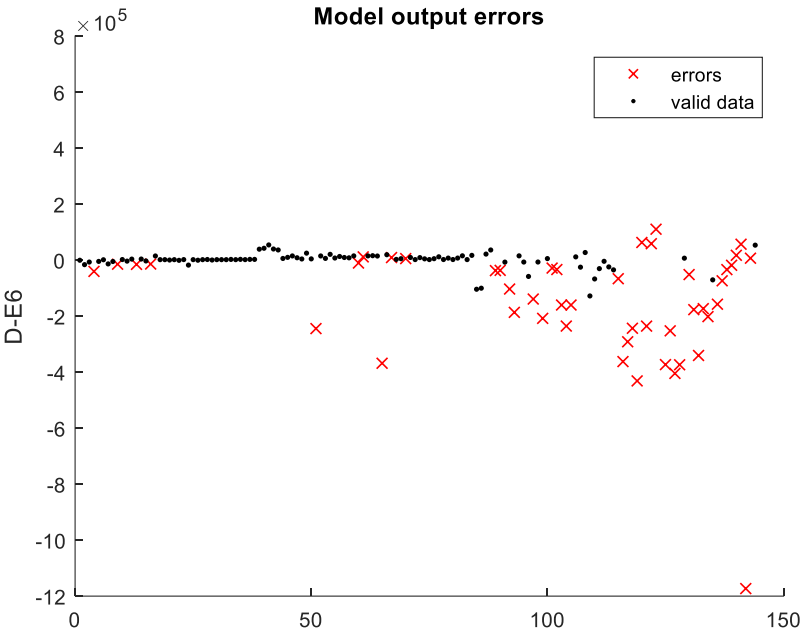
Figure 4.   Example error run. Original duration was 24h, but the run ended at 11h.
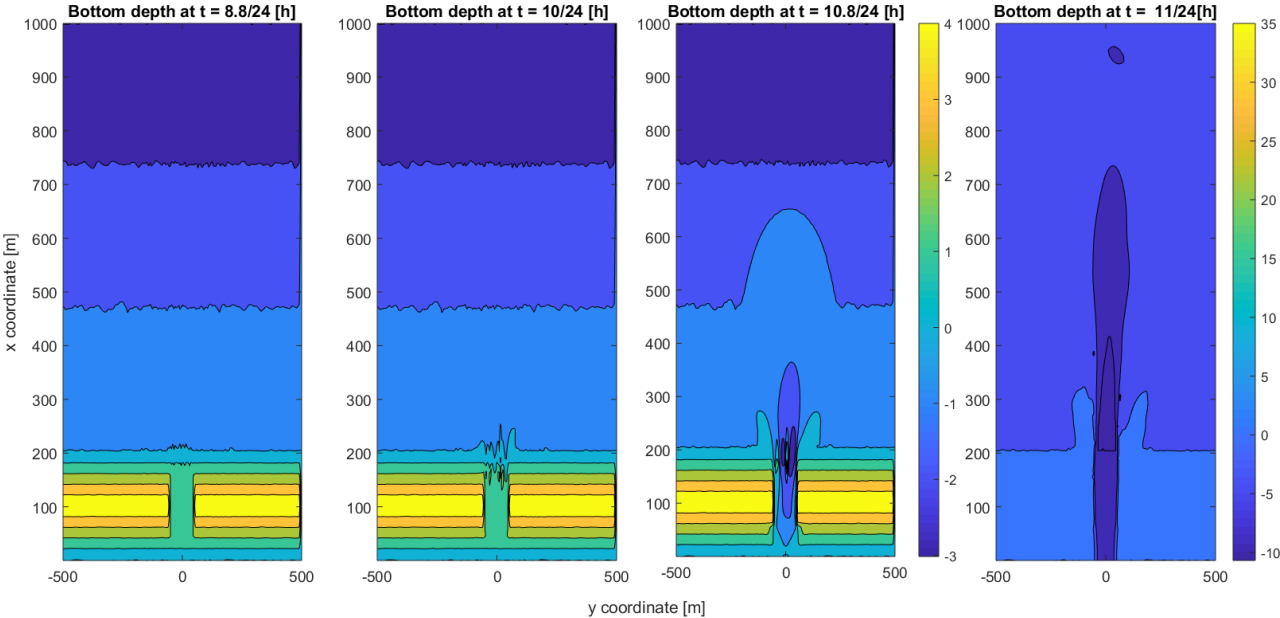
Appendix 2.1

Table 1. Variables per run (only stable runs).

Run number	Elevation	Duration	Slope	Cover	Water level difference	Island width	D-E	Storm output, based on D-E
1	1	6	0,015	1	2,5	400	-638,037	inlet
2	1	6	0,00875	1	3,5	400	-16327,7	inlet
3	1	6	0,015	1	3	400	-7117,24	inlet
5	1	9	0,0075	1	3	400	-4801,67	inlet
6	1	9	0,0075	1	2,5	400	1095,158	washover
7	1	9	0,00875	1	3,5	400	-13751,6	inlet
8	1	12	0,015	1	3	400	-5127,63	inlet
10	1	12	0,0075	1	2,5	400	1878,634	washover
11	1	18	0,015	1	3	400	-3773,64	inlet
12	1	18	0,0075	1	2,5	400	3443,334	washover
14	1	24	0,0075	1	2,5	400	4677,663	washover
15	1	24	0,015	1	3	400	-2119,51	inlet
17	2	18	0,015	1	3,5	200	14633,2	washover
18	2	3	0,00875	1	3	400	1455,218	washover
19	2	3	0,00625	1	2,5	400	1437,637	washover
20	2	3	0,0075	1	3,5	400	99,8302	washover
21	2	3	0,0125	1	2,1	400	1443,425	washover
22	2	6	0,015	1	3,5	400	-953,37	inlet
23	2	6	0,0125	1	3	400	1716,559	washover
24	2	6	0,015	1	4,5	400	-17977,4	inlet
25	2	6	0,0125	1	2,5	400	1482,628	washover
26	2	9	0,015	1	3,5	400	-582,347	inlet
27	2	9	0,0125	1	2,5	400	1442,175	washover
28	2	12	0,015	1	3	400	1973,36	washover
29	2	12	0,00625	1	3,5	400	174,7027	washover

30	2	12	0,0125	1	2,5	400	1470,6	washover
31	2	18	0,00625	1	3,5	400	1464,631	washover
32	2	18	0,00625	1	2,5	400	1449,685	washover
33	2	18	0,0175	1	3	400	2330,152	washover
34	2	24	0,00625	1	2,5	400	1444,165	washover
35	2	24	0,0125	1	3	400	3084,65	washover
36	2	24	0,00875	1	3,5	400	3877,387	washover
37	1	18	0,015	0,01	3,5	200	2458,977	washover
38	1	18	0,00625	0,01	2,5	200	2411,205	washover
39	1	12	0,0175	0,01	2,5	400	38873,35	washover
40	1	18	0,0075	0,01	2,5	400	42135,15	washover
41	1	24	0,00875	0,01	2,5	400	33635,02	washover
42	2	6	0,0125	0,01	3	200	39519,84	washover
43	2	6	0,0125	0,01	2,5	200	6659,511	washover
44	2	9	0,00625	0,01	2,5	200	5716,328	washover
45	2	12	0,0075	0,01	2,5	200	9657,18	washover
46	2	18	0,0075	0,01	2,5	200	14736,55	washover
47	2	24	0,0125	0,01	2,5	200	81006,87	washover
48	2	3	0,00875	0,01	2,5	400	3903,601	washover
49	2	3	0,00625	0,01	3	400	24713,48	washover
50	2	6	0,00625	0,01	2,5	400	4228,746	washover
52	2	6	0,0125	0,01	3	400	14651,03	washover
53	2	9	0,00875	0,01	2,5	400	5918,397	washover
54	2	9	0,0075	0,01	3	400	20433,45	washover
55	2	12	0,00625	0,01	2,5	400	7267,925	washover
56	2	12	0,0125	0,01	3	400	12840,02	washover
57	2	18	0,0225	0,01	2,5	400	9132,388	washover
58	2	24	0,00625	0,01	2,5	400	10874,91	washover
62	1	6	0,0125	1	2,5	200	14934,57	washover
63	1	9	0,0175	1	2,5	200	15597,78	washover
64	1	9	0,0125	1	3	200	14423,94	washover

66	1	12	0,0225	1	2,5	200	19071,78	washover
68	2	6	0,015	1	2,5	200	2366,559	washover
69	2	6	0,00625	1	3	200	4864,499	washover
71	2	6	0,0125	1	3,5	200	9265,333	washover
72	2	9	0,00525	1	2,5	200	1724,518	washover
73	2	9	0,0125	1	3,5	200	8783,943	washover
74	2	9	0,00625	1	3	200	4330,217	washover
75	2	12	0,00625	1	2,5	200	1772,034	washover
76	2	12	0,00625	1	3	200	4923,93	washover
77	2	12	0,0075	1	3,5	200	11663,92	washover
78	2	18	0,0175	1	2,5	200	1911,13	washover
79	2	18	0,00625	1	3	200	7073,226	washover
80	2	24	0,015	1	2,5	200	2051,376	washover
81	2	24	0,00625	1	3	200	9335,881	washover
82	2	24	0,00625	1	3,5	200	16689,9	washover
83	2	9	0,00625	1	3	400	1694,516	washover
84	1	6	0,0175	0,01	2,5	200	16761,9	washover
85	1	6	0,00875	0,01	3,5	200	-104189	inlet
86	1	6	0,00875	0,01	3	200	-100443	inlet
87	1	9	0,0075	0,01	2,5	200	21357,03	washover
88	1	9	0,0075	0,01	4,5	200	36004,61	washover
91	1	12	0,00875	0,01	2,5	200	-7336,39	inlet
94	1	18	0,015	0,01	3	200	15062,59	washover
95	1	24	0,0125	0,01	3	200	12194,97	washover
96	1	24	0,00875	0,01	3,5	200	17470,96	washover
98	1	24	0,00875	0,01	2,5	200	15732,37	washover
100	1	3	0,00625	0,01	2,5	400	5242,667	washover
106	1	6	0,01125	0,01	2,5	400	11400,3	washover
107	1	9	0,0175	0,01	3	400	-25388	inlet
108	1	9	0,0125	0,01	2,5	400	26962,12	washover
109	1	9	0,015	0,01	3,5	400	-128167	inlet

110	1	12	0,01125	0,01	3,5	400	-67458,2	inlet
111	1	12	0,00875	0,01	3	400	-30593,4	inlet
112	1	18	0,00625	0,01	3	400	-4409,58	inlet
113	1	18	0,0075	0,01	3,5	400	-24419,3	inlet
114	1	24	0,0125	0,01	3,5	400	13837,15	washover
129	2	3	0,00875	0,01	3,5	400	6728,432	washover
135	2	18	0,0175	0,01	3	400	-70700,6	inlet
144	1	24	0,0075	1	2,5	200	57466,03	washover

Appendix 2.2

Table 2. Variables per run (only unstable runs).

Run number	Elevation	Duration	Slope	Cover	Water level difference	Island width	D-E	Storm output, based on D-E
4	1	6	0.0175	1	4.5	400	-40473.5	inlet
9	1	12	0.0225	1	3.5	400	-14709.6	inlet
13	1	18	0.0245	1	3.5	400	-15332.4	inlet
16	1	24	0.0175	1	3.5	400	-13688.3	inlet
51	2	6	0.0225	0.01	4.5	400	-244676	inlet
59	2	24	0.00875	0.01	3	400	-79503.7	inlet
60	1	6	0.0225	1	3.5	200	-10615	inlet
61	1	6	0.0175	1	3	200	11320.02	washover
65	1	9	0.01125	1	3.5	200	-368482	inlet
67	1	12	0.01125	1	3	200	8889.727	washover
70	2	6	0.0175	1	4.5	200	5293.91	washover
89	1	9	0.00875	0.01	3.5	200	-37762.1	inlet
90	1	9	0.01125	0.01	3	200	-36739.1	inlet
92	1	12	0.00875	0.01	3.5	200	-103420	inlet
93	1	12	0.0175	0.01	3	200	-186724	inlet
97	1	24	0.00875	0.01	4.5	200	-62661.6	inlet
99	1	3	0.00875	0.01	4.5	400	-208181	inlet
101	1	3	0.015	0.01	3	400	-28536.5	inlet
102	1	3	0.015	0.01	3.5	400	-33855.1	inlet
103	1	6	0.0175	0.01	3.5	400	-160494	inlet
104	1	6	0.0075	0.01	4.5	400	-235633	inlet
105	1	6	0.00875	0.01	3	400	-160494	inlet
115	1	24	0.0175	0.01	3	400	-14179.9	inlet
116	2	6	0.0225	0.01	3.5	200	-362478	inlet
117	2	6	0.015	0.01	4.5	200	-291754	inlet

118	2	9	0.0175	0.01	3.5	200	-243497	inlet
119	2	9	0.01125	0.01	4.5	200	-431525	inlet
120	2	9	0.00875	0.01	3	200	62810.11	washover
121	2	12	0.01125	0.01	3.5	200	-235788	inlet
122	2	12	0.0075	0.01	3	200	58446.68	washover
123	2	18	0.015	0.01	3	200	110241.1	washover
124	2	18	0.0075	0.01	3.5	200	604370.7	washover
125	2	24	0.015	0.01	4.9	200	22666.85	washover
126	2	24	0.00875	0.01	3	200	11430.26	washover
127	2	24	0.00625	0.01	4.5	200	23463.06	washover
128	2	24	0.0175	0.01	3.5	200	12755.11	washover
130	2	3	0.00875	0.01	4.5	400	-51798.5	inlet
131	2	6	0.0175	0.01	3.5	400	-177017	inlet
132	2	9	0.0075	0.01	3.5	400	-340676	inlet
133	2	12	0.0075	0.01	3.5	400	-173464	inlet
134	2	18	0.00875	0.01	3.5	400	-202008	inlet
136	2	24	0.0225	0.01	3.5	400	3272.9	washover
137	1	6	0.00875	1	4.5	200	-74025.5	inlet
138	1	12	0.0175	1	3.5	200	-34069.6	inlet
139	1	18	0.0125	1	3.5	200	-18613.9	inlet
140	1	18	0.0075	1	3	200	17099.12	washover
141	1	18	0.0175	1	2.5	200	56635.15	washover
142	1	24	0.0125	1	3.5	200	12828.07	washover
143	1	24	0.015	1	3	200	14526.79	washover

Appendix 3

Table 3. Variables per Sandy observation

	Island width	coordinates	Island height	Island cover	Storm duration	Washover size	Water level difference	Water slope	Storm output
Sandy 1	300	40° 2'23.51"N 74° 3'1.41"W	5.57	1	12	0	3.3	0.0110	inlet
Sandy 2	286	40° 3'2.20"N 74° 2'52.15"W	6.07	1	12	0	3.1	0.0108	inlet
Sandy 3	280	40° 4'26.15"N 74° 2'33.02"W	5.23	1	12	532	1.5	0.0054	washover
Sandy 4	281	40° 4'21.72"N 74° 2'34.18"W	5.23	1	12	235	1.5	0.0053	washover
Sandy 5	142	40° 8'17.52"N 74° 1'33.78"W	4.99	0	12	0	0.4	0.0025	inlet
Sandy 6	129	40°10'51.24"N 74° 0'41.91"W	3.76	0	12	0	0.7	0.0054	inlet
Sandy 7	343	39°49'57.89"N 74° 5'22.90"W	4.66	0	12	232	2.4	0.0070	washover
Sandy 8	232	39°31'43.16"N 74°16'12.96"W	2.22	0	9	582	0.5	0.0022	washover
Sandy 9	267	39°31'39.44"N 74°16'17.39"W	2.22	0	9	138	0.5	0.0019	washover
Sandy 10	283	39°30'42.84"N 74°17'9.89"W	2.11	0	9	1322	0.5	0.0018	washover
Sandy 11	433	39° 1'41.99"N 74°46'47.34"W	2.03	0	6	0	0.0	0.0000	inlet
Sandy 12	84	39° 6'56.82"N 74°42'56.90"W	2.92	1	6	935	0.0	0.0000	washover
Sandy 13	177	39°26'3.73"N 74°20'5.67"W	2.32	0	9	1622	0.0	0.0000	washover

Sandy 14	948	39°56'43.94"N 74° 4'27.50"W	3.64	1	12	2576	3.0	0.0032	washover
Sandy 15	761	39°58'8.55"N 74° 4'13.39"W	5.58	1	12	256	3.7	0.0049	washover
Sandy 16	631	39°58'24.07"N 74° 4'5.79"W	6.07	1	12	805	3.7	0.0059	washover
Sandy 17	645	39°58'21.85"N 74° 4'6.42"W	5.58	1	12	1293	3.7	0.0057	washover
Sandy 18	667	39°58'34.51"N 74° 4'4.76"W	6.07	1	12	80	3.7	0.0055	washover
Sandy 19	305	40° 0'27.85"N 74° 3'31.12"W	6.34	1	12	79	3.7	0.0121	washover
Sandy 20	260	40° 0'35.20"N 74° 3'28.19"W	6.34	1	12	205	3.7	0.0142	washover
Sandy 21	242	40° 2'25.86"N 74° 2'59.80"W	5.57	1	12	800	3.3	0.0136	washover
Sandy 22	226	40° 2'44.26"N 74° 2'55.11"W	5.71	1	12	517	3.3	0.0146	washover
Sandy 23	240	40° 2'45.42"N 74° 2'55.08"W	5.71	1	12	266	3.3	0.0138	washover
Sandy 24	261	40° 3'3.95"N 74° 2'51.60"W	6.07	1	12	172	3.3	0.0126	washover
Sandy 25	267	40° 3'5.92"N 74° 2'51.15"W	6.07	1	12	238	3.3	0.0124	washover
Sandy 26	203	40°13'48.26"N 73°59'47.75"W	4.28	1	12	311	0.3	0.0012	washover
Sandy 27	258	40°40'2.11"N 73° 3'20.58"W	4.49	0	18	1261	2.3	0.0089	washover
Sandy 28	257	40°43'19.92"N 72°53'58.69"W	4.15	0	18	1927	2.4	0.0093	washover

Sandy 29	271	40°43'24.20"N 72°53'45.64"W	2.03	0	18	0	2.4	0.0089	inlet
Sandy 30	234	40°43'52.66"N 72°52'15.24"W	4.24	0	18	1598	2.1	0.0090	washover